International Journal of Pharmaceutics 446 (2013) 112–118

Contents lists available at SciVerse ScienceDirect

International Journal of Pharmaceutics

journal homepage: www.elsevier.com/locate/ijpharm

Glutathione-mediated drug release from Tiopronin-conjugated gold nanoparticles for acute liver injury therapy

Quan-Ying Bao[a,b], Dong-Dong Geng[a,b], Jing-Wei Xue[b], Geng Zhou[a], Shen-Yang Gu[a], Ya Ding[a,*], Can Zhang[b,**]

[a] College of Pharmacy, China Pharmaceutical University, Nanjing 210009, China
[b] Center of Drug Discovery, State Key Laboratory of Natural Medicines, China Pharmaceutical University, Nanjing 210009, China

ARTICLE INFO

Article history:
Received 5 November 2012
Received in revised form 21 January 2013
Accepted 30 January 2013
Available online 14 February 2013

Keywords:
Gold conjugates
Tiopronin
Pharmacokinetics
Passive target
Acute liver injury
Drug delivery

ABSTRACT

Tiopronin-conjugated gold nanoparticles (TPN@GNPs), with glutathione (GSH)-responsive drug release property, were developed for acute liver injury therapy. The TPN@GNPs were prepared using a one-pot synthesis method and characterized by UV–vis and transmission electronic microscopy methods. The TPN@GNPs displayed typical surface plasmon resonance of nanogold with a narrow size distribution (*ca.* 2 nm). The *in vitro* drug release profiles of the conjugates indicated that TPN@GNPs were able to release TPN in a sustained fashion for 4 h at a simulated intracellular level of GSH. pH values or ionic strengths of the release media had no obvious influence on TPN release from the surface of nanoparticles. The pharmacokinetic studies in rats showed that the TPN@GNPs had longer MRT (7.71 h) than TPN (3.96 h), indicating sustained release pattern of TPN@GNPs *in vivo*. The sustained release of TPN at the relative high GSH concentration could ameliorate the instability of TPN and enable the drug release in the target cells. Although the IC_{50} value of TPN@GNPs with TPN/$AuCl_4^-$ of 3:1 (mol/mol) showed slight increase in comparison with that of the free TPN in HepG2 cells (1.26 ± 1.07 *vs.* 1.73 ± 1.16 mg/mL), the TPN@GNPs displayed better effects over TPN in the treatment of acute liver injury *in vivo*. In a liver injury mice model induced by CCl_4, the histological analysis showed both the TPN@GNPs and free TPN group could repair the liver injury. In addition, the biochemical parameters showed TPN@GNPs could reduced the aminotransferase to a lower level compared with TPN, which might be due to the sustained drug release and passive liver targeting properties of TPN@GNPs. It demonstrated that gold nanoparticle-based drug delivery system allowed smart functions and superior properties by taking advantages of the unique small size effects and surface chemical properties.

© 2013 Elsevier B.V. All rights reserved.

1. Introduction

Gold nanoparticles (GNPs) have attracted tremendous attentions in the field of drug delivery due to shape- and size-controllable preparation methods (Schmid, 1992), high drug loading capacity (Templeton et al., 1999a,b; Gibson et al., 2007), and the ability to utilize the enhanced permeability and retention (EPR) effect to passively target drugs to tumor cells or inflammatory cells *via* the leaky vasculature (Ghosh et al., 2008). Moreover, GNPs-based drug delivery system (DDS) also possesses the following unique and attractive advantages for drug delivery applications such as the easy surface modification through the place-exchange reaction and thiol chemistry (Templeton et al., 1999a), excellent light scattering signal for image-guided drug delivery (Boisselier and Astruc, 2009), toxicity-free and inert gold core for safe cell and small animal studies (Khlebtsov and Dykman, 2011; Tsoli et al., 2005; Bhattacharya and Mukherjee, 2008; Connor et al., 2005), and light-mediated hyperthermia combined with chemotherapy for the cancer treatment. Up to now, various therapeutics (*e.g.* small molecules, biomacromolecules, and diagnostic probes) have been loaded on the surface of gold nanoparticles *via* the physical adsorption, electrostatic interaction, specific recognition, as well as S—Au covalent bonds (Ghosh et al., 2008; Boisselier and Astruc, 2009; Duncan et al., 2010).

Most recently, triggered-release drug delivery systems based on gold nanoparticles have been developed, in which drug release can be triggered *via* a variety of stimulations such as low pH in tumor tissue (Wang et al., 2011), photo- and thermal-stimulations (Vivero-Escoto et al., 2009), and intracellular high level of glutathione (GSH) (Hong et al., 2006; Navath et al., 2008; Kim et al., 2012). Among them, due to the wide application of thiol chemistry in GNPs-based drug delivery system, GSH-sensitive drug release attracts more attentions (Hostetler et al., 1998) and offers

* Corresponding author. Tel.: +86 25 83271090; fax: +86 25 83271090.
** Corresponding author. Tel.: +86 25 83271171; fax: +86 25 83271171.
E-mail addresses: ayanju@163.com (Y. Ding), zhangcan@cpu.edu.cn (C. Zhang).

0378-5173/$ – see front matter © 2013 Elsevier B.V. All rights reserved.
http://dx.doi.org/10.1016/j.ijpharm.2013.01.073

great potential to design intracellular GSH-responsive drug delivery system. Some model fluorescent molecules conjugated on the surface of gold nanoparticles have been investigated for the glutathione-mediated delivery and release studies (Hong et al., 2006; Chompoosor et al., 2008). Based on the related mechanism, drug@gold conjugates will not release the free drugs until they penetrate into cells since the exchange of thiol-containing drug by GSH requires a relatively high level of GSH (1–10 mM for intracellular GSH concentration *vs.* 2 μM for extracellular GSH level) (Hassan and Rechnitz, 1982). That is to say, the GSH-mediated release drug delivery system will be able to avoid early release of the medicine prior to entering the target cells, which can subsequently reduce the toxicity arising from the wide distribution of medicine.

N-(2-mercaptopropionyl) glycine (Tiopronin, TPN), containing a thiol group, has been used as a hepatoprotectant clinically for years in China. The chemical structure of this compound is shown in Fig. 1. Commercially available dosage forms of TPN are conventional injections, immediate release tablets, and enteric-coated tablets. However, the instability and toxicity of TPN have hampered its clinical application (Cao et al., 2009). Due to the presence of high reactive thiol group, TPN can be easily oxidized to form disulfates in the environment (Huang et al., 2009). Therefore, TPN injection is often prepared and diluted prior to administration and the time for infusion is limited within 1 h, which makes it extremely difficult for the clinical use (Cao et al., 2009). In addition, the current TPN formulations on the market are not able to target to the liver, which might be responsible for anaphylaxis, severe allergic side effect associated with conventional TPN formulations.

In this work, to solve the current problems for the practical application of TPN and improve its hepatoprotective effect, TPN was conjugated on the surface of gold nanoparticles *via* S—Au covalent bonds to form a smart drug delivery system in the nanoscale (denoted as TPN@GNPs). TPN@GNP conjugates were synthesized by a simple one-pot method as shown in Fig. 1. The thiol group in TPN structure is passivated on the surface of gold nanoparticles to avoid the oxidation reaction. Taking advantage of small size of GNPs, TPN molecules grafted on gold surface can passively target to liver tissue, where the lesion site lies (Khlebtsov and Dykman, 2011). In addition, the GSH-mediated TPN release will ensure that TPN molecules are released freely inside cells by ligand exchange at a high level of GSH, subsequently leading to reduction in the toxicity of TPN. TPN@GNP conjugates prepared in this work were well-characterized. The *in vitro* cell toxicity and the TPN release behavior of TPN@GNP conjugates have been studied. The *in vivo* pharmacokinetics studies of TPN and TPN@GNPs were carried out in rats. In order to evaluate the therapeutic efficacy of the conjugate against the acute liver injury in mice, the model was induced by CCl_4 and TPN@GNP conjugates were administered *via* intravenous injection, using free TPN with the same drug dosage as the control. The results displayed that the therapy efficacy of the GSH-triggered TPN@GNP conjugates was much better than that of the conventional injection, based on the introduction of unique and superior properties from gold nanoparticles and the rational design of their stimuli-responsive release function.

2. Materials and methods

2.1. Materials and instruments

Hydrogen tetrachloroaurate hydrate ($HAuCl_4{\cdot}3H_2O$) was obtained from Shanghai Chemical Regent Company (China). Tiopronin (TPN, 96%) was purchased from TCI Development Co., Ltd. (China). Unless otherwise stated, all starting materials were obtained from commercial suppliers and used without further purification. All aqueous solutions were prepared using deionized water (>18 MΩ, Purelab Classic Corp., USA).

UV–vis spectra were recorded on a UV-2401 PC UV/Vis spectrophotometer (Shimadzu, USA). A single drop of TPN@GNPs solution was deposited on a TEM grid and then dried in air, which was imaged with a JEM-2100 TEM with acceleration voltages of 200 kV (JEOL JEM, Japan). The thermo gravimetric analysis (TGA) was carried out on a thermal gravimetric analyser (TG 209 F1, Netzsch, Germany).

2.2. Synthesis of GNPs and TPN@GNPs

All the glassware used in our experiments were treated with aqua regia and cleaned with purified water. Citrate-protected GNPs were prepared by the method describes elsewhere (Daniel and Astruc, 2004). Briefly, 150.1 mg sodium citrate and 1.845 mL (5×10^{-5} mol/L) $HAuCl_4$ aqueous solution were added into 25 mL of purified water in a baker with magnetic stirring in an ice bath. 3 mg sodium borohydride was added into 25 mL of purified water in another baker with magnetic stirring in an ice bath. After 20 min, the later mixture in the baker was poured into the former baker slowly, the color of the cocktail turned to wine red. After another 20 min, the citrate-protected GNPs were collected for use.

The one-pot synthesis method was employed to prepare TPN@GNPs (Templeton et al., 1999b) with some modification. Briefly, TPN and $HAuCl_4{\cdot}3H_2O$ with the molar ratio of 1:1, 3:1, and 5:1 were dissolved in a certain amount of methanol/acetic acid mixture solvent (6:1, v/v) to keep the concentration of TPN to be 11.2 mg/mL. Sodium borohydride was added in the mixture and stirred vigorously for 15 min at 44 °C. The obtained dark brown suspension was stirred for 30 min after its cooling to room temperature. The solvent was removed under vacuum at 35 °C, and the crude TPN@GNPs were obtained. To purify the conjugates, the crude TPN@GNPs were dissolved in water and dialyzed (MWCO = 10,000 Da) against deionized water for 24 h. The purified solution was lyophilized and kept at 4 °C for further use.

2.3. In vitro drug release studies

0.1 mL of TPN@GNPs aqueous solution (0.13 g/mL) was placed in a dialysis tube (MWCO = 10,000 Da), in which 0.9 mL of release media (PBS buffers with or without 10 mM GSH) was added. After sealed tightly at each end with cable ties, the dialysis tubes were immersed into 10 mL of release media in a beaker, stirring at 37 ± 0.5 °C. The release media used were 50 mM PBS (pH 5.5 and pH 7.4) with different the ionic strengths (ranging from zero to 1.0 M). At predetermined time points, 200 μL of samples were withdrawn and replenished with 200 μL of fresh release media. All the samples were performed in triplicates.

A reversed-phase HPLC with UV detection was selected to analyze TPN. The HPLC system was Shimadzu LC-20A series (Shimadzu Corporation, Japan), consisting of a quaternary pump, a vacuum degasser, an auto-sampler, a thermostated column compartment, and an analytical column (Phecda, ODS, 250 mm × 4.6 mm, ID 5 μm; Hanbon Sci. & Tech Co., Ltd., China). According to the UV–vis absorption spectra of TPN, UV detection wavelength was set at 210 nm. The column temperature was maintained at 30 °C with isocratic elution at a flow rate of 1.0 mL/min and the injection volume was 20 μL. The mobile phase consisted of acetonitrile and aqueous KH_2PO_4 (10 mM, adjusted to pH 3.2 with phosphoric acid) (5/95, v/v).

2.4. Cell culture and viability tests

HepG2 cell lines were grown in the Dulbecco's modified Eagle medium (DMEM, Thermo Fisher Scientific Inc., China) supplemented with 10% fetal bovine serum and 1% penicillin and streptomycin at 37 °C with 5% CO_2. To determine the IC_{50} values of TPN and TPN@GNPs, the HepG2 cells were plated into 96-well

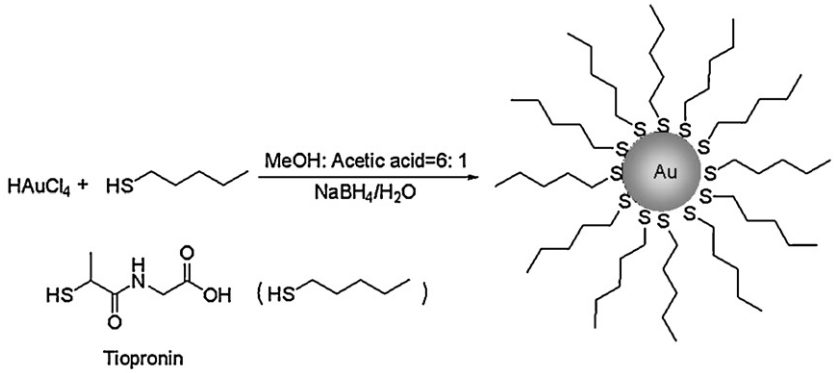

Fig. 1. Chemical structure of TPN and schematic synthesis of TPN@GNP conjugates.

plates and incubated overnight. After 24 h, the medium was replaced with fresh DMEM containing different concentrations of TPN@GNPs or free TPN and further incubated for 24 h. Then, PBS and MTT solution were added, incubating at 37 °C for 4 h. And DMSO was added to dissolve the MTT formazan and the absorbance was measured on a microplate reader (Multiskan MK3, Thermo Fisher Scientific Inc., USA) at 570 nm and corrected at 630 nm.

2.5. Pharmacokinetics study in rats

2.5.1. Study design

Male rats weighed 200–250 g were divided into two groups ($n = 4$) and administered with TPN solution and TPN@GNPs conjugates (18 mg/kg) *via* tail vein injection, respectively. 0.5 mL of blood samples were withdrawn from retro orbital sinus at 0.83, 0.17, 0.33, 0.5, 1, 2, 3, 4, 6, 8, 10, and 12 h after injection. The blood samples were collected in heparinized tubes and centrifuged at 3000 rpm for 5 min to obtain plasma samples and stored at −20 °C until assay.

2.5.2. Sample preparation

For a 100 μL aliquot of each plasma sample, 20 μL of methanol, 10 μL of internal standard solution (25 μg/mL Fudosteine in methanol), 10 μL of L-Cysteine (20 μg/mL), and 10 μL 1,4-Dithiothreitol (3 mg/mL) were added and vortex mixed for 30 s. After incubated in a water bath at 30 °C for 10 min, the samples were deproteinized by 200 μL of methanol, vortex mixed for 3 min and centrifuged at 15,000 rpm for 10 min. 20 μL of the supernatant of each sample was injected for LC–MS/MS analysis.

2.5.3. LC–MS/MS analysis

The chromatographic separation was performed on a RP-HPLC column (ZORBAX Eclipse Plus C18, 2.1 mm × 150 mm, 3.5 μm, Agilent Technologies, USA). The column temperature was maintained at 30 °C with an isocratic elution at a flow rate of 0.3 mL/min and the injection volume was 20 μL. The mobile phase consisted of methanol and 0.1% formic acide (10/90, v/v).

The HPLC (Agilent 1290 Infinity series, USA) was connected to the mass spectrometry (MS/MS, Agilent 6460 triple quadrupole, USA) equipped with an electrospray interface (ESI) operating in a negative-ion mode. The assay was carried out using multiple-reaction monitoring (MRM) with the transition from m/z 162.0 → 74.0 for TPN and m/z 178.0 → 91.0 for the IS. The source parameters were as follows: gas temperature, 350 °C; gas flow, 7 L/min; nebulizer, 30 psi; capillary voltage, 3.5 kV.

The plasma pharmacokinetic parameters were estimated by Kinetica (4.4 version, Thermo Electron Corporation) software for both TPN and TPN@GNPs injections.

2.6. Efficacy of TPN@GNPs against acute liver injured mice

2.6.1. Model construction of acute liver injury in mice

Healthy male ICR mice (body weight 18–22 g) used in the experiment were purchased from Zhejiang Experimental Animal Center (Certificate number: SCXK (Zhe) 20080033). The mice were randomly divided into five groups (ten mice per group) and administrated with saline, saline, TPN solution, TPN@GNPs, and free GNPs with the same TPN dosage (26 mg/kg) *via* tail vein injection for seven consecutive days. After 2 h of the last administration, except the first group (as the control), the mice were treated with 0.1% CCl_4 peanut oil (v/v) *via* intraperitoneal administration (10 mL/kg of body weight) to induce acute liver injury in mice. 16 h after the administration of CCl_4, the blood samples were collected and the livers were excised, washed with saline and weighed.

2.6.2. Biochemical parameters of hepatic function

The relative liver weight percentage was calculated by liver weight dividing the body weight of a mouse. The animotranferase activities, aspartate aminotransferase (AST) and alanine aminotransferase (ALT) levels in the serum were measured using diagnostic kits (Nanjing Jiancheng Institute of Biotechnology). Origin soft ware (Version 8.6) was selected to address the data.

2.6.3. Histological analysis

The excised livers were weighed and was fixed with 4% paraformaldehyde. The samples were processed and sectioned, and the thin tissue sections were stained with hematoxylin and eosin (H and E) and Masson trichrome for histological observation (Olympus TH4-200, Olympus Optical Co., Ltd., Japan).

2.7. Statistics

All the results are presented as mean ± SD. The data were analyzed by one-way analysis of variance (ANOVA) with the appropriate Bonferroni correction to determine the significant differences for multiple comparisons. Significance was assumed at $P < 0.05$.

3. Results and discussion

3.1. Synthesis and characterization of TPN@GNPs

The TPN@GNPs was prepared by the one-step reduction method of $HAuCl_4$ by sodium borohydride in the presence of stabilizer of TPN (Templeton et al., 1999b). The as-prepared TPN@GNPs (with TPN/$AuCl_4^-$ reaction molar ratio of 1:1, 3:1, and 5:1) were characterized with UV-Vis absorption spectroscopy. As shown in Fig. 2, the surface plasmon resonance (SPR) band of all TPN@GNPs samples

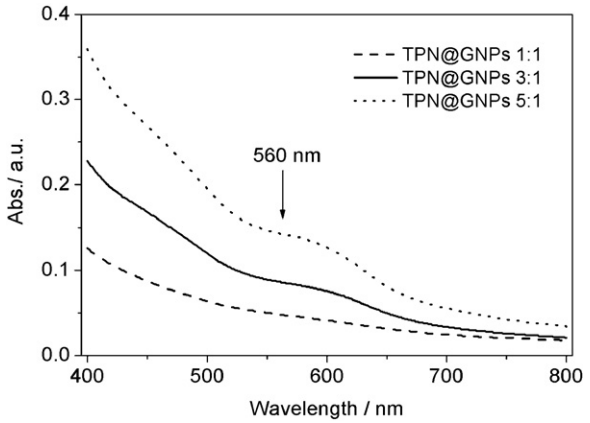

Fig. 2. UV–vis absorption spectra of TPN@GNPs solutions with TPN/$AuCl_4^-$ molar ratio of 1:1, 3:1, and 5:1.

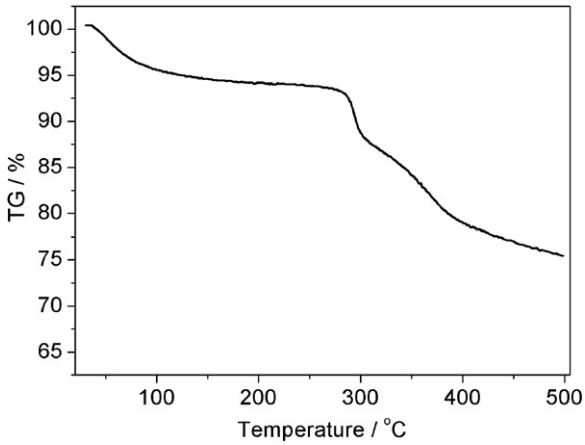

Fig. 4. TGA curve of TPN@GNPs with TPN/$HAuCl_4$ molar ratio of 3:1.

was displayed at 560 nm, which was a little red-shifted comparing with that of gold nanoparticles protected by the citrate salt (not shown here). This red-shift was due to the successful formation of S—Au bonds on the gold surface. It was found that with the increase of molar ratio of TPN/$AuCl_4^-$, the UV–vis absorption of TPN@GNPs increased and the sample with molar ration of 5:1 showed the highest SPR band at 560 nm. However, we found that the TPN@GNPs (5:1) sample in the solution was quite unstable and some black precipitation can be found when its freeze-dried sample was resuspended in the deionized water. While TPN@GNPs samples with other TPN/$AuCl_4^-$ reaction molar ratios were clear solutions when resuspended in the deionized water, and the TPN@GNPs solution kept unchanged for a long time such as several months. For the comprehensive consideration of high stability and TPN loading in TPN@GNPs samples, TPN@GNPs with TPN/$AuCl_4^-$ reaction molar ratio of 3:1 was chosen for the further studies.

TEM assay has been carried out to characterize the size and shape of the TPN@GNPs. As shown in Fig. 3, TPN@GNPs showed spherical structure with a narrow distribution (the diameter of *ca.* 2 nm), which was consistent with the UV–vis results demonstrated in Fig. 2. From the TEM image, it can be found that all particles displayed a spherical shape and were well-dispersed.

To evaluate the number of TPN molecules modified on the surface of gold nanoparticles (Hostetler et al., 1998; Roger, 1995), TGA has been performed and the result was shown in Fig. 4. The organic ligands on the GNP surface decompose to volatile disulfides at a gradually rising temperature. While for gold it possesses a high melting point that is robust enough to undergo the high temperatures applied in the TGA process and leave as the elemental gold residues after thermal analysis process. It can be seen in Fig. 4 that he weight fraction of TPN molecules passivated on the surface of TPN@GNPs is about 24% and therefore the number of TPN molecules modified on the surface of gold nanoparticles can be accurately calculated to be 463 (Daniel and Astruc, 2004). This result was consistent with that of the TPN assay *via* HPLC, conducted by dialysis in a high concentration (50 mM) of GSH in 10 mL of water.

3.2. In vitro release study of TPN from TPN@GNPs

In vitro release testing of TPN from the TPN@GNPs was operated with or without GSH (10 mM) in the release media. Since the content of TPN was not detectable in the release media even after 6 h in the absence of GSH (not shown here), Fig. 5 shows the drug release results in the presence of 10 mM GSH. Firstly, pH influence was evaluated, and the release behavior of TPN in the release media of PBS at pH 5.5 and pH 7.4 was shown in Fig. 5A. Although it was found that different pH values of release media slightly affected the accumulative release of TPN, the TPN release rate was comparatively faster in a higher pH 7.4 *vs.* pH 5.5. The mechanism of drug release from the TPN@GNPs was related to thiol group exchange reaction, in which GSH functioned as a reducing agent to exchange TPN molecules from the surface of TPN@GNPs. The reduction activity of GSH was relevant to the number of its thiol groups. Since the pKa value of GSH was about 8.8 and its thiolate form had much higher reduction activity than that of its thiol form, relative higher pH value of release media would lead to rapid ligand exchange rate, and subsequent the release rate of TPN from TPN@GNPs surface (Winterbourn and Metodiewa, 1999). Therefore, it could be concluded that GSH was a sensitive trigger for drug release from the

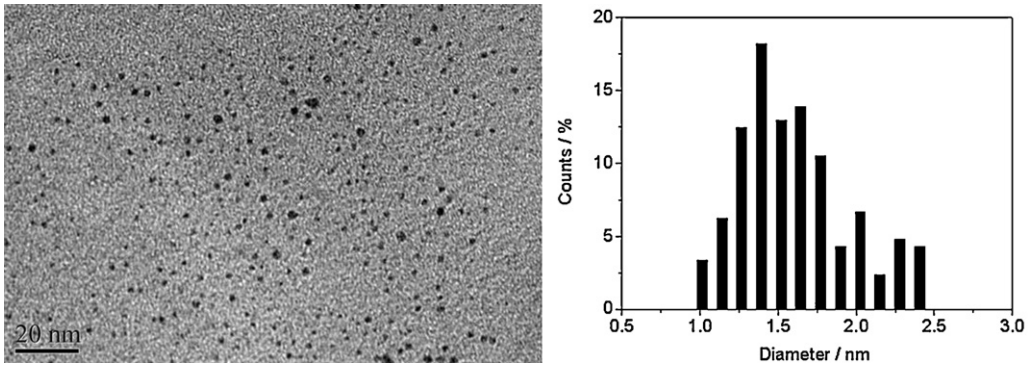

Fig. 3. TEM image of TPN@GNPs with TPN/$AuCl_4^-$ molar ratio of 3:1.

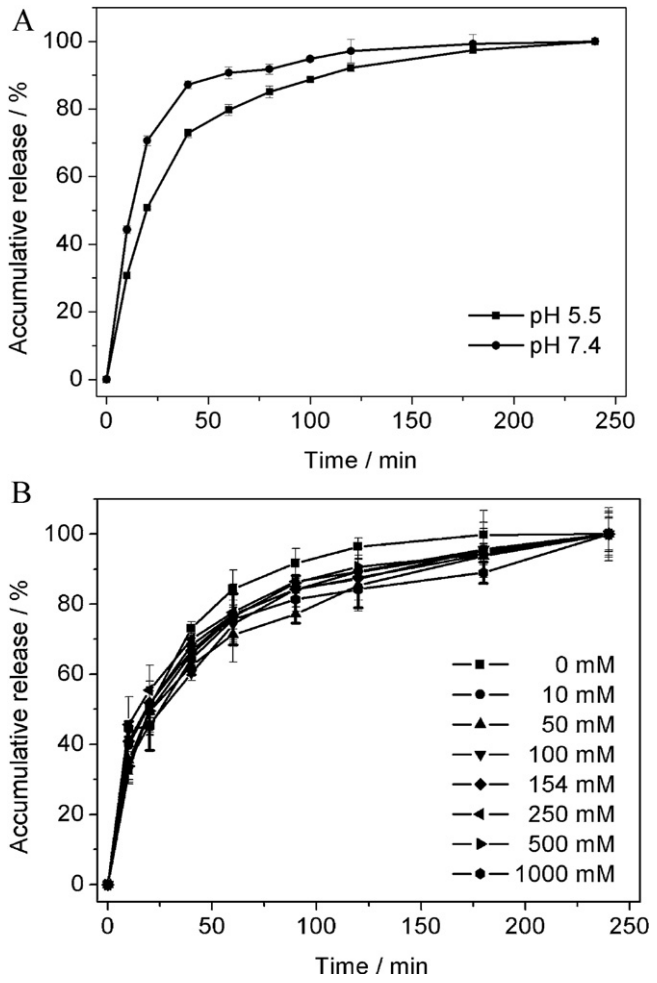

Fig. 5. The drug release profiles of TPN from the conjugate (A) in PBS at pH 5.5 and 7.4 ($n = 3$, mean ± SD) and (B) in release media with different ionic strength (NaCl solution with ionic concentration in the range of 0–1 M).

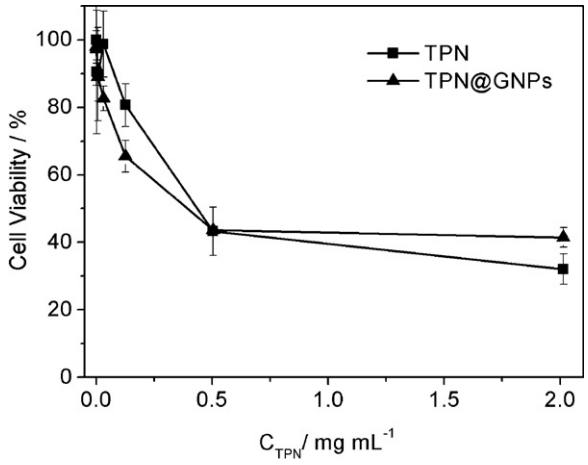

Fig. 6. Cell viability of HepG2 cells incubated with TPN@GNPs and TPN after 24 h at 37 °C.

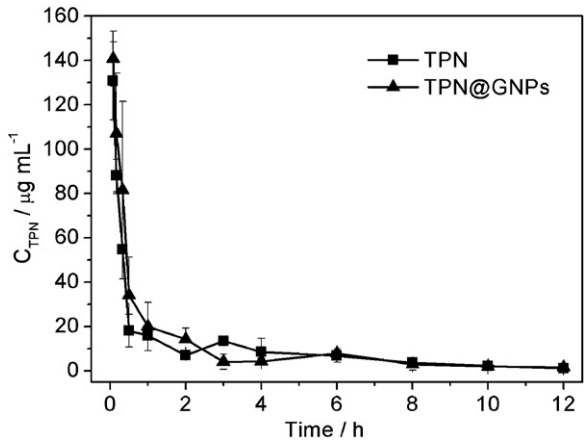

Fig. 7. The mean plasma concentration–time profiles of TPN and TPN@GNPs following intravenous administration at a dose of 18 mg/kg in rats (mean ± SD, $n = 4$).

TPN@GNPs conjugate, especially in the interior of the cell and at the physiological pH, and the release profiles displayed a sustained release pattern within 4 h.

As shown in Fig. 5B, ionic strength did not show significant influence on the release rate of TPN from the TPN@GNPs. Within the ionic strength studied, TPN release rate slightly decreased with the increasing ionic strength. The process of drug release from the conjugate was synchronized with the process of GSH adsorbing on GNPs (Lim et al., 2008).

3.3. Cell viability

The cytotoxicity of TPN@GNPs is a vital parameter to apply the gold conjugate *in vivo*, so the MTT assay was carried out in both the free TPN and the TPN@GNPs containing the same amount of TPN. In view of the chromatic interference of the conjugate, the cell viability in previous reports were determined by the method of direct counting the cell numbers (Cai et al., 2011) or using the Cell Counting Kit-8 (CCK-8 assay) (Huang et al., 2012) to avoid the disturbance. Due to 3-(4,5)-dimethylthiahiazo(-z-y1)-3,5-diphenytetrazoliumromide (MTT) has no absorption at 630 nm, MTT assay performed in this work was adopted to determine the cell viability by calculating the absorption differences at 570 nm and 630 nm. As shown in Fig. 6, the IC_{50} values of the TPN@GNPs and TPN on the HepG2 cell line were 1.26 ± 1.07 and 1.73 ± 1.16 mg/mL, respectively, indicating that the TPN@GNPs was relatively safe.

3.4. Pharmacokinetics study in rats

The mean plasma concentration–time curves of free TPN and TPN@GNPs were shown in Fig. 7 and main pharmacokinetic parameters were summarized in Table 1. The mean retention time (MRT) of TPN@GNPs was significantly longer than that of free TPN (7.714 h *vs.* 3.962 h), indicating that TPN release from TPN@GNPs *in vivo* was in a sustained manner. The *in vivo* result was consistent with the *in vitro* drug release profiles discussed earlier in this paper. In addition, the TPN from TPN@GNPs was eliminated considerably

Table 1
The pharmacokinetic parameters of TPN following the administration of free TPN and TPN@GNPs in rats (mean ± SD, $n = 4$).

Parameters	TPN	TPN@GNPs
MRT (h)	3.962 ± 1.182*	7.714 ± 2.142
$AUC_{0-\tau}$ (h μg/mL)	103.985 ± 26.819	111.232 ± 13.323
$t_{1/2\beta}$ (h)	2.746 ± 1.739*	9.796 ± 2.844
V_d (mL)	0.196 ± 0.127	0.330 ± 0.217
Cl (mL/h/mg)	0.0468 ± 0.0172	0.0407 ± 0.0206

MRT: mean retention time; $AUC_{0-\tau}$: area under curve from 0 h to 12 h; $t_{1/2\beta}$: elimination half-life; V_d: apparent distribution volume; Cl: clearance rate.

* $P < 0.05$ compared with TPN@GNPs.

slowly *in vivo* with a larger $t_{1/2\beta}$ of 9.796 h. It could be deduced from the prolonged MRT and $t_{1/2\beta}$ that TPN@GNPs could ameliorate the instability and rapid elimination of TPN *in vivo*. Other parameters such as V_d, Cl, and $AUC_{0-\tau}$ showed no significance between TPN and its GNP conjugates.

3.5. *In vivo* assessment of TPN@GNPs on acute liver injured mice induced by CCl_4

Based on the above studies, TPN@GNP conjugate proved to be able to release the free TPN in a sustained way under a GSH stimulated condition. To better understand the practical superiority of TPN@GNP conjugate comparing to the free TPN, it is necessary to evaluate the treatment efficacy of hepatitis for TPN@GNP formulation *in vivo*. In the animal experiment, acute liver injury model in mice was constructed by administering the animals intraperitoneally with carbon tetrachloride (CCl_4). The hepatic markers of acute liver injury were determined, including the relative liver weight (LW) percentage, AST, and ALT activity levels shown in

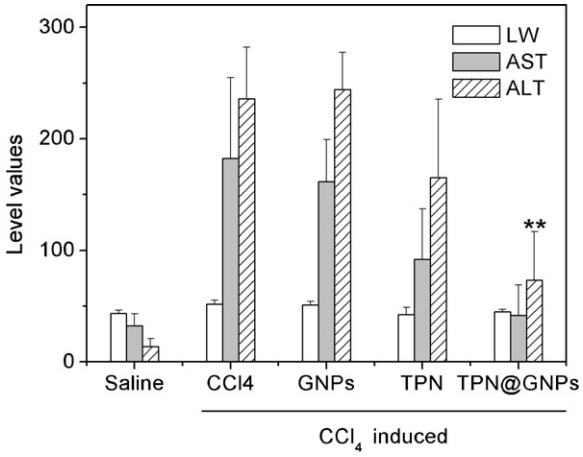

Fig. 8. Effects of the TPN and TPN@GNPs on the relative LW percentage, AST and ALT activity. Each of the data was presented as mean ± SD, and $^{**}P < 0.01$ represented the significance of inter groups.

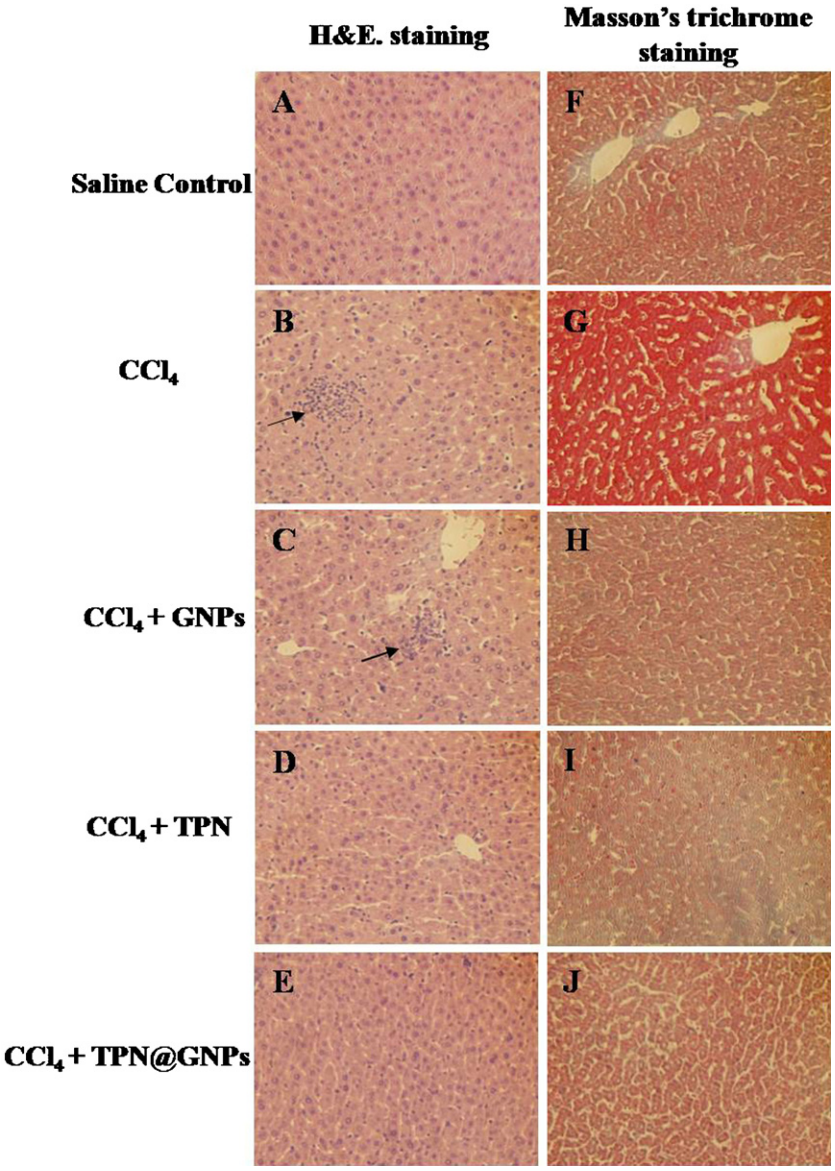

Fig. 9. Histological analysis of liver slices for the five groups of mice after treatment. The images on the left column (A–E) are H and E staining, and on the right are Masson's trichrome staining (F–J). All the images were captured by the Olympus microscope at a 400× magnification of the original images. The arrows represented the abnormal state of the liver, especially the inflammation.

Fig. 8, respectively. The relative LW is calculated by the following formula:

$$\text{Relative LW} = \text{liver weight (mg)}/\text{body weight (g)} \times 100\%$$

Compared to the control group, the CCl_4 group resulted in significant increasing of the relative LW as well as the AST, and ALT activity, which implied that the acute live injury model in mice was successfully established. There was no significant difference between the citrate-protected GNPs and CCl_4 group in LW, AST, and ALT activities, which means that the GNPs themselves did not enhance or attenuate the efficacy of liver injury. In the CCl_4 induced groups, both TPN and TPN@GNP groups could significantly reduce the elevated relative LW and AST activity caused by CCl_4 to the normal level. Although there was no significance between two groups, the TPN@GNP group showed lower AST activity level in comparison with that of TNP group, which indicated better recovery of liver function using TPN@GNPs. In addition, compared with TPN group, the effect of TPN@GNPs on reducing ALT activity was of significant difference ($P < 0.01$, Fig. 8), which could be due to the TPN accumulation in liver *via* the passive targeting of gold nanoparticles and GSH-mediated TPN release after the conjugates were uptake by liver cells.

The images of liver sections stained with H and E or Masson's trichrome were presented in Fig. 9. In this study, the liver injury was not serious according to the experimental design, so the Masson's trichrome staining (Fig. 9F–J) showed no fibrosis in all the experimental groups. However, in the H and E stained tissues, compared with the saline group, the CCl_4 (Fig. 9B) and GNP (Fig. 9C) group appeared obvious inflammation and abnormal structure of liver cells (marked by arrows). While the free TPN (Fig. 9D) and its GNP conjugates (Fig. 9E) could restore the impaired liver cells to normal state, without inflammation and structure abnormalities. The histological analysis of five groups was in accordance with the results of the biochemical parameters of hepatic function.

4. Conclusion

In summary, TPN-conjugated gold nanoparticles were prepared by using a one-pot synthesis method, and characterized by UV–vis, TEM, and TGA measurements. The *in vitro* studies suggest the conjugate was GSH-sensitive and free TPN could release from the conjugate completely in a sustained manner at the presence of intracellular level of GSH. The pharmacokinetics study showed TPN@GNPs could improve the pharmaceutics of free TPN and sustain the drug release *in vivo*, in consistency with the results of drug release *in vitro*. Although, compared with that of free TPN, the cell cytotoxicity of TPN@GNPs on the HepG2 cell line was slightly increased, the sustained drug release behavior and passive liver targeting property of TPN@GNP conjugates render them a better therapeutic efficiency on acute liver injure therapy than that of the conventional injection. The TPN@GNPs could substantially reduce the rising aminotranferase ALT caused by CCl_4 to the normal level. Compared to the conventional preparation, the TPN@GNPs possessed greater advantages in delivering drug to targeted cells and preventing liver from acute injury. From this study, there is a huge potential of applying the drug-loaded GNPs to clinical use and this novel drug delivery system will be notably promising in the upcoming future.

Acknowledgments

This work was financially supported by the Natural Science Foundation of China (30900337), the Doctoral Fund of Ministry of Education of China (20090096120001), the Fundamental Research Funds for the Central Universities (JKP2011008), the Qing Lan Project, and the Program for New Century Excellent Talents in University (NCET-10-0816).

References

Bhattacharya, R., Mukherjee, P., 2008. Biological properties of naked metal nanoparticles. Adv. Drug Deliv. Rev. 60, 1289–1306.
Boisselier, E., Astruc, D., 2009. Gold nanoparticles in nanomedicine: preparations imaging, diagnostics, therapies and toxicity. Chem. Soc. Rev. 38, 1759–1782.
Cai, X., Chen, H.H., Wang, C.L., Chen, S.T., Lai, S.F., Chien, C.C., Chen, Y.Y., Kempson, I.M., Hwu, Y.K., Yang, C.S., Margaritondo, G., 2011. Imaging the cellular uptake of tiopronin-modified gold nanoparticles. Anal. Bioanal. Chem. 401, 809–816.
Cao, Y.H., Yang, H., Li, G.H., Wang, J.B., 2009. Study on relationship between the stability of Tiopronin and adverse reaction. Chin. Pharm. J. 44, 842–844.
Chompoosor, A., Han, G., Rotello, V.M., 2008. Charge dependence of ligand release and monolayer stability of gold nanoparticles by biogenic thiols. Bioconjugate Chem. 19, 1342–1345.
Connor, E.E., Mwamuka, J., Gole, A.M., Murphy, C.J., Wyatt, M.D., 2005. Gold nanoparticles are taken up by human cells but do not cause acute cytotoxicity. Small 1, 325–327.
Daniel, M.C., Astruc, D., 2004. Gold nanoparticles: assembly, supramolecular chemistry, quantum-size-related properties, and applications toward biology catalysis, and nanotechnology. Chem. Rev. 104, 293–346.
Duncan, B., Kim, C., Rotello, V.M., 2010. Gold nanoparticle platforms as drug and biomacromolecule delivery systems. J. Control. Release 148, 122–127.
Ghosh, P., Han, G., De, M., Kim, C.K., Rotello, V.M., 2008. Gold nanoparticles in delivery applications. Adv. Drug Deliv. Rev. 60, 1307–1315.
Gibson, J.D., Khanal, B.P., Zubarev, E.R., 2007. Paclitaxel-functionalized gold nanoparticles. J. Am. Chem. Soc. 129, 11653–11661.
Hassan, S.S.M., Rechnitz, G.A., 1982. Determination of glutathione and glutathione-reductase with a silver sulfide membrane-electrode. Anal. Chem. 54, 1972–1976.
Hong, R., Han, G., Fernández, J.M., Kim, B.J., Forbes, N.S., Rotello, V.M., 2006. Glutathione-mediated delivery and release using monolayer protected nanoparticle carriers. J. Am. Chem. Soc. 128, 1078–1079.
Hostetler, M.J., Wingate, J.E., Zhong, C.J., Harris, J.E., Vachet, R.W., Clark, M.R., Londono, J.D., Green, S.J., Stokes, J.J., Wignall, G.D., Glish, G.L., Porter, M.D., Evans, N.D., Murray, R.W., 1998. Alkanethiolate gold cluster molecules with core diameters from 1.5 to 5.2 nm: core and monolayer properties as a function of core size. Langmuir 14, 17–30.
Huang, J., Yin, Y.J., Huang, H.W., Zhang, Q.M., Hang, T.J., 2009. Determination of tiopronin injection and its related substances in Tiopronin injection by HPLC. Chin. Pharm. J. 44, 1108–1111.
Huang, K., Ma, H., Liu, J., Huo, S., Kumar, A., Wei, T., Zhang, X., Jin, S., Gan, Y., Wang, P.C., He, S., Zhang, X., Liang, X.J., 2012. Size-dependent localization and penetration of ultrasmall gold nanoparticles in cancer cells, multicelluar spheroids, and tumors in vivo. ACS Nano 6, 4483–4493.
Khlebtsov, N., Dykman, L., 2011. Biodistribution and toxicity of engineered gold nanoparticles: a review of in vitro and in vivo studies. Chem. Soc. Rev. 40, 1647–1671.
Kim, M., Seo, J.H., Jeon, W.I., Kim, M.Y., Cho, K., Lee, S.Y., Joo, S.W., 2012. Real-time monitoring of anticancer drug release in vitro and in vivo on titania nanoparticles triggered by external glutathione. Talanta 88, 631–637.
Lim, I.I.S., Mott, D., Ip, W., Njoki, P.N., Pan, Y., Zhou, S., Zhong, C.J., 2008. Interparticle interactions in glutathione mediated assembly of gold nanoparticles. Langmuir 24, 8857–8863.
Navath, R.S., Kurtoglu, Y.E., Wang, B., Kannan, S., Romero, R., Kannan, R.M., 2008. Dendrimer–drug conjugates for tailored intracellular drug release based on glutathione levels. Bioconjugate Chem. 19, 2446–2455.
Roger, H., 1995. Monolayers in three dimensions: NMR, SAXS, thermal, and electron hopping studies of alkanethiol stabilized gold clusters. J. Am. Chem. Soc. 117, 12537–12548.
Schmid, G., 1992. Large clusters and colloids Metals in the embryonic state. Chem. Rev. 92, 1709–1727.
Templeton, A.C., Wuelfing, W.P., Murray, R.W., 1999a. Monolayer-protected cluster molecules. Acc. Chem. Res. 33, 27–36.
Templeton, A.C., Cliffel, D.E., Murray, R.W., 1999b. Redox and fluorophore functionalization of water-soluble, tiopronin-protected gold clusters. J. Am. Chem. Soc. 121, 7081–7089.
Tsoli, M., Kuhn, H., Brandau, W., Esche, H., Schmid, G., 2005. Cellular uptake and toxicity of Au 55 clusters. Small 1, 841–844.
Vivero-Escoto, J.L., Slowing, I.I., Wu, C.W., Lin, V.S., 2009. Photoinduced intracellular controlled release drug delivery in human cells by gold-capped mesoporous silica nanosphere. J. Am. Chem. Soc. 131, 3462–3463.
Wang, F., Wang, Y.C., Dou, S., Xiong, M.H., Sun, T.M., Wang, J., 2011. Doxorubicin-tethered responsive gold nanoparticles facilitate intracellular drug delivery for overcoming multidrug resistance in cancer cells. ACS Nano 5, 3679–3692.
Winterbourn, C.C., Metodiewa, D., 1999. Reactivity of biologically important thiol compounds with superoxide and hydrogen peroxide. Free Radic. Biol. Med. 27, 322–328.